Journal of Photochemistry and Photobiology A: Chemistry 204 (2009) 32–38

Contents lists available at ScienceDirect

Journal of Photochemistry and Photobiology A: Chemistry

journal homepage: www.elsevier.com/locate/jphotochem

Synthesis, spectroscopic and electrochemical properties of the perylene–tetrathiafulvalene dyads

Yu Zhang [a], Zheng Xu [b], Hai-xiao Qiu [a], Guo-qiao Lai [b], Yong-jia Shen [a,*]

[a] Laboratory for Advanced Materials and Institute of Fine Chemicals, East China University of Science and Technology, Shanghai 200237, PR China
[b] Key Lab of Organosilicon Chemistry and Material Technology of Ministry of Education, Hangzhou Normal University, Hangzhou 310012, PR China

ARTICLE INFO

Article history:
Received 1 November 2008
Received in revised form 4 January 2009
Accepted 2 February 2009
Available online 3 March 2009

Keywords:
Perylene
TTF
Fluorescence spectra
Intramolecular charge transfer
Electron transfer

ABSTRACT

The TTF–perylene dyads **1–3** were designed and synthesized. The absorption spectra, cyclic voltammogram (CV) of dyads and the frontier orbital calculation indicated no intramolecular charge transfer (ICT) interaction in their ground state. The fluorescence spectra and theoretical calculation of the dyads **1–3** revealed the photoinduced electron transfer (PET) interaction existed in the dyads in their excited state. The chemical oxidation implied an effective reverse electron transfer from the perylene* to the TTF^{2+} species. The three donor–acceptor systems could be used as models for the study of photoinduced electron transfer and reverse electron transfer process.

1. Introduction

Perylene and its derivatives have been widely studied in material science due to their high molar absorptivity, high fluorescence quantum yields together with excellent photochemical and thermal stability [1–5]. This chromophore has also attracted considerable attention on account of its optical and electrochemical properties [6,7] and the perylene derivatives have been applied in various fields [8,9].

On the other hand, tetrathiafulvalene (TTF) and its derivatives feature unique π-donor properties and the possibility of exploiting these multistage redox states (TTF^0, $TTF^{\bullet+}$, TTF^{2+}) have been intensively investigated. As a result of progress in synthetic TTF chemistry, TTFs have been incorporated into a number of macrocyclic and supramolecular systems in order to create new functional materials with desired structures, stability, and physical properties [10–12]. As a consequence, many efforts have been devoted to the preparation of a variety of the covalent linkage of the TTFs and an electron acceptor counterpart [13], for instance the TTF–anthrancene triads [14,15]. However, the TTF–perylene systems have been rarely investigated. Leroy-Lhez et al. [16] and D.B. Zhu and co-workers [17] reported the TTF–perylene diimide molecular systems respectively, and the diimide was used as the linkage in all these systems.

Hence, we set our target to merge TTF and perylene moieties (Fig. 1) and the donor–σ-acceptor systems (Fig. 2) could be formed as the perylene with a low-lying HOMO level compared to TTF. Herein, we reported the synthesis of the TTF–perylene dyads **1–3** (Schemes 1 and 2), their spectroscopic and electrochemical properties.

2. Experimental section

2.1. Chemicals and instruments

All chemicals were purchased commercially and the solvents dried or distilled when necessary using standard procedures. ^1H NMR and ^{13}C NMR were obtained on a Bruker AVANCE 500 spectrometer operating at 500 and 100 MHz: chemical shifts were quoted downfield of TMS. Elemental analyses were obtained from an Elementar vario ELIII C, H, N analyzer and their results were found to be in good agreement with the calculated values. UV–vis spectra were recorded on a CARY 100 Conc UV–vis spectrophotometer. The fluorescence spectra were recorded on a CARY Eclipse Fluorescence spectrophotometer and were corrected for the spectral response of the machines. The fluorescence lifetime experiment was performed on Edinburgh steady state and time resolved fluorescence spectrometers FL 900. All the electrochemical experiments were performed in dichloromethane with *n*-Bu_4NPF_6 as the supporting electrolyte, platinum as the working and counter electrodes, and Ag/AgCl as the reference electrode. The scan rate was 50 mV/s.

* Corresponding author. Tel.: +86 21 64252967; fax: +86 21 64252967.
E-mail address: yjshen@ecust.edu.cn (Y.-j. Shen).

1010-6030/$ – see front matter © 2009 Elsevier B.V. All rights reserved.
doi:10.1016/j.jphotochem.2009.02.016

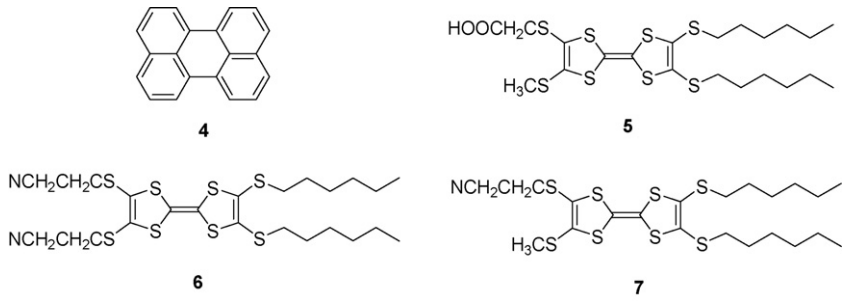

Fig. 1. The structures of perylene **4** and TTFs **5–7**.

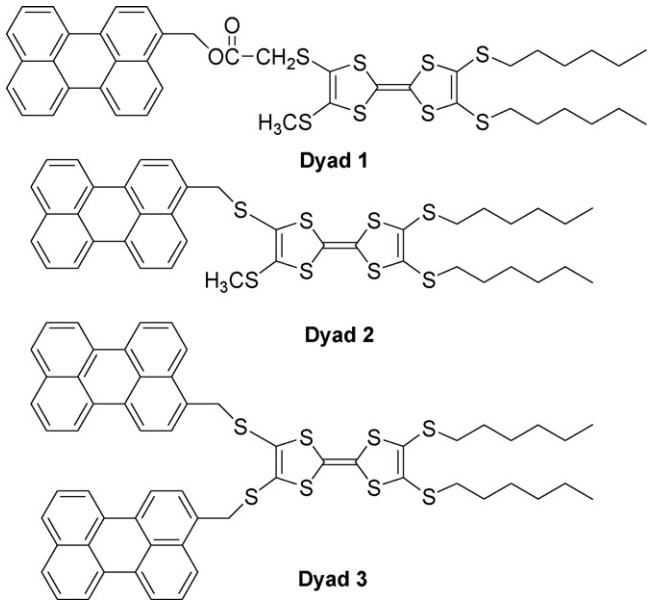

Fig. 2. The structures of TTF–perylene dyads **1–3**.

2.2. Molecular orbital calculations

Quantum mechanical calculations were performed on an SGI Altix 450 sever using Gaussian 03 package [18]. All geometries were initially optimized with MM2 method combined in ChemBioOffice 2008 with default set, and then by the semi-empirical AM1 method. The obtained optimized geometries were finally re-optimized with ab initio HF method at 6-31g level. The frontier orbitals were depicted with 0.01 isocontour based on HF/6-31g level.

2.3. Synthesis

2.3.1. Dyad *1*

To a suspension of TTF–CO_2H **5** (288 mg, 0.5 mmol) in dried CH_2Cl_2 (15 mL) were added successively dicyclohexylcarbodiimide (DCC) (113 mg, 0.55 mmol), 4-(dimethylamino)pyridine (DMAP) (61 mg, 0.5 mmol), 1-hydroxybenzotriazole (HOBT) (68 mg, 0.5 mmol) and perylene **8** (141 mg, 0.5 mmol) under nitrogen atmosphere. The reaction mixture was stirred at room temperature for 48 h and the reaction mixture turned from yellow brown to a ginger-yellow color. After removed the solvent under reduced pressure, the residue was purified by column chromatography on silica gel (CH_2Cl_2/petroleum ether, 1:2, v/v) and dyad **1** (217 mg,

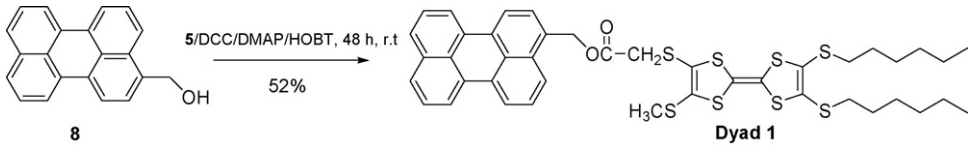

Scheme 1. Synthesis of dyad **1**.

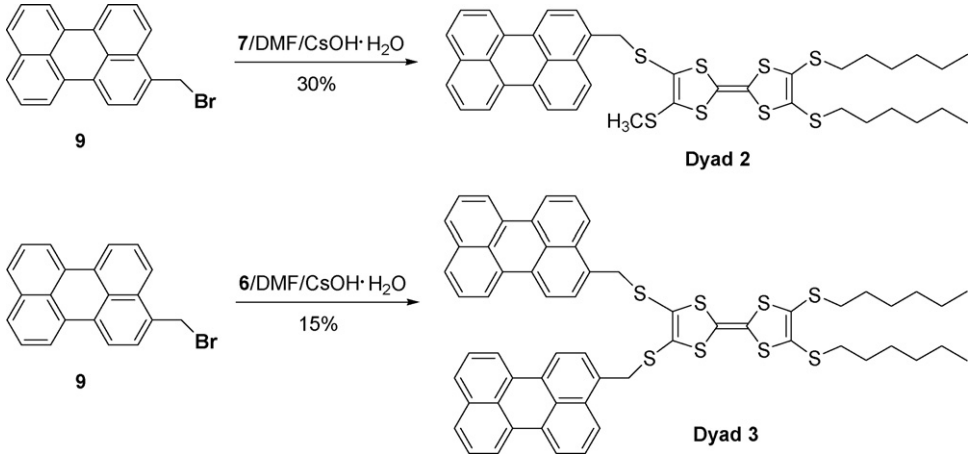

Scheme 2. Synthesis of dyads **2** and **3**.

52% yield) was isolated as ginger-yellow solid. mp 135–137 °C; δ_H ($CDCl_3$, 500 MHz) 8.27–8.08 (4H, m, Ar–H), 7.81–7.76 (1H, m, Ar–H), 7.63–7.61 (2H, m, Ar–H), 7.52–7.49 (2H, m, Ar–H), 7.43–7.39 (2H, m, Ar–H), 5.52 (2H, s, Ar–CH_2), 3.15 (2H, s, S–CH_2–), 2.78-2.72 (4H, t, *J* 7.2 Hz, S–CH_2–), 2.26 (3H, s, S–CH_3), 1.55–1.49 (4H, m, alkyl-H), 1.11–1.30 (12H, m, alkyl-H), 0.81–0.77 (6H, t, *J* 6.2 Hz, alkyl-CH_3); δ_C ($CDCl_3$, 100 MHz) 168.7, 134.6, 131,2, 131.0, 129.0, 128.6, 128.4, 128.0, 127.8, 126.8, 126.6, 123.6, 120.4, 120.2, 119.7, 64.5, 32.3, 31.3, 29.7, 28.2, 22.5, 19.0, 14.0; found: C, 60.02, H, 5.33. $C_{42}H_{44}S_8O_2$ requires C, 60.25, H, 5.30%; *m*/*z* (ESI^+): 837.7 $[M+1]^+$.

2.3.2. Dyad **2**

To a solution of compound **7** (0.567 g, 1 mmol) in anhydrous degassed DMF (50 mL) was added a solution of $CsOH{\cdot}H_2O$ (0.168 g, 1.05 mmol) in absolute degassed MeOH (8 mL) over a period of 30 min. The mixture was stirred for the additional 30 min, then bromomethylperylene **9** (0.345 g, 1 mmol) in anhydrous DMF (20 mL) was introduced and orange compound started to precipitate. The mixture was stirred for an additional 12 h. The precipitate was filtered and washed with MeOH (3 × 10 mL), and dried. The crude product was purified by column chromatography on silica gel (CH_2Cl_2/petroleum ether, 1:2, v/v) and dyad **2** (0.23 g, 29.6% yield) was obtained as orange powder. mp 107–110 °C; δ_H ($CDCl_3$, 500 MHz) 8.30–8.15 (4H, m, Ar–H), 7.92 (1H, d, *J* 7.8 Hz, Ar–H), 7.71 (2H, d, *J* 8.2 Hz, Ar–H), 7.64 (1H, t, *J* 7.9 Hz, Ar–H), 7.56–7.51 (3H, m, Ar–H), 4.95 (2H, s, alkyl-H), 2.82 (t, 4H, *J* 7.3 Hz, S–CH_2–), 2.46 (3H, s, S–CH_3), 1.72–1.58 (4H, m, alkyl-H), 1.46–1.42 (4H, m, alkyl-H), 1.30–1.25 (8H, m, alkyl-H), 0.88 (t, 6H, *J* 6.2 Hz, alkyl-CH_3); δ_C ($CDCl_3$, 100 MHz) 134.6, 131,2, 131.0, 129.0, 128.7, 128.4, 128.0, 127.9, 126.8, 126.6, 123.6, 120.4, 120.3, 119.7, 36.3, 31.3, 29.7, 28.2, 22.5, 19.0, 14.0; found: C, 61.57; H, 5.45. $C_{40}H_{42}S_8$ requires: C, 61.65; H, 5.43; *m*/*z* (ESI^+): 778.3 $[M^+]$.

2.3.3. Dyad **3**

To a solution of compound **6** (0.303 g, 1 mmol) in anhydrous degassed DMF (30 mL) was added a solution of $CsOH{\cdot}H_2O$ (0.326 g, 2.10 mmol) in anhydrous degassed MeOH (10 mL) over a period of 30 min. The mixture was stirred for an additional 30 min, whereupon bromomethylperylene **9** (0.690 g, 2 mmol) in anhydrous DMF (20 mL) was introduced and the orange crude product started to precipitate. After stirring for 16 h, the precipitate was filtered and washed with MeOH (3 × 10 mL), dried. Then, the orange solid was purified by column chromatography on silica gel (CH_2Cl_2/petroleum ether, 1:2, v/v) and dyad **3** (0.078 g, 15.2% yield) was obtained as orange powder. mp 134–138 °C; δ_H ($CDCl_3$, 500 MHz) 8.28–8.13 (4H, m, Ar–H), 7.96 (1H, d, *J* 7.8 Hz, Ar–H), 7.71 (2H, d, *J* 8.2 Hz, Ar–H), 7.64 (1H, t, *J* 7.9 Hz, Ar–H), 7.56 (1H, d, *J* 7.6 Hz, Ar–H); 7.51 (2H, m, Ar–H), 4.95 (2H, s, alkyl-H), 2.82 (t, 4H, *J* 7.3 Hz, S–CH_2–), 1.72–1.58 (4H, m, alkyl-H), 1.46–1.42 (4H, m, alkyl-H), 1.30–1.25 (8H, m, alkyl-H), 0.88 (6H, t, *J* 6.2 Hz, alkyl-CH_3); δ_C ($CDCl_3$, 100 MHz) 134.6, 131,2, 131.1, 129.0, 128.7, 128.4, 128.0, 127.9, 126.8, 126.6, 123.6, 120.4, 120.3, 120.8, 36.3, 31.3, 29.7, 28.1, 22.5, 14.0; found: C, 70.12; H, 5.11. $C_{60}H_{52}S_8$ requires: C, 69.99; H, 5.09; *m*/*z* (ESI^+): 1028.6 $[M^+]$.

3. Results and discussion

3.1. Synthesis

Our target is to synthesize a kind of the dyads consisted of TTF and perylene, expecting them will exhibit unique photo/electrochemical properties. However, directly linking these two moieties is impossible, because of no reactive groups in the molecules. A reasonable covalent bridge between them is needed. Based on the synthetic TTF chemistry, cyanoethyl groups in TTFs, *i.e.* TTFs **6** and **7**, can be deprotected by caesium hydroxide monohydrate ($CsOH{\cdot}H_2O$) to afford TTF thiolates, which can be trapped by the appropriate electrophlie (usually RX, R = alkyl, CH_2Ph, X = I, Br, Cl) to form the expected TTF derivatives [19–21]. According to this reaction, TTFs **6** and **7**, with long alkyl chains, were designed and synthesized. Simultaneously, bromomethylperylene **9** [22,23] was synthesized and used as an alkylation reagent. TTF **6** or **7** reacted with perylene **9** in dried DMF in the presence of one equivalent or two equivalent of $CsOH{\cdot}H_2O$ to form dyads **2** and **3** (Scheme 2), respectively. Thus, two dyads were obtained, which linked with the same thioether group between the TTF and perylene. They exhibited good solubility in normal organic solvents. In order to compare the internal interactions of dyads linked with different covalent bridges, for example, a longer flexible ester linkage, we synthesized the TTF **5** with a carboxyl functional group [24] and a hydroxymethyl substituted perylene **8**, expecting them to exhibit more efficient photoinduced charge-separation with long lifetime radical ion-pair [25]. Through the esterification reaction between **5** and **8** by using dicyclohexylcarbodiimide as the coupling reagent together with 4-(dimethylamino)pyridine and 1-hydroxybenzotriazole, dyad **1** with ester group as linkage was obtained (Scheme 1). Further, we attempted to synthesize a perylene derivative with two hydroxymethyl groups, as well as TTF with two carboxyl groups and to achieve the TTF–perylene polymer. Unfortunately, it failed.

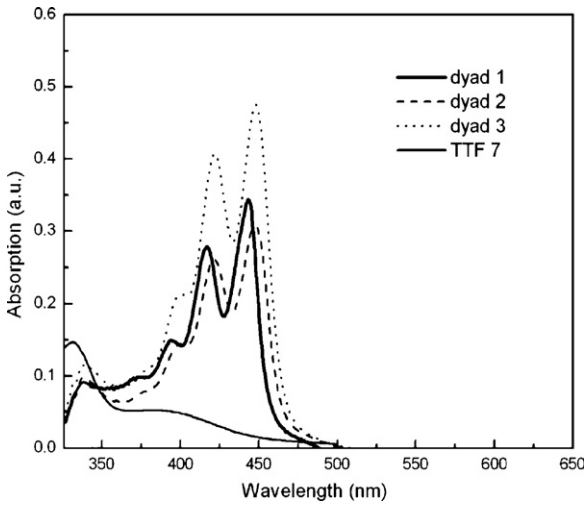

Fig. 3. The absorption spectra of dyads **1**, **2** and **3** (1×10^{-5} M) in CH_2Cl_2.

3.2. Electronic absorption

The UV–vis absorption spectra of dyads **1–3** and TTF **7** in CH_2Cl_2 were shown in Fig. 3 and the maximum absorption wavelengths were listed in Table 1, respectively. The maximum absorption wavelength of perylene **4** was also presented in Table 1 as reference. For the dyads, all of them showed two strong absorption bands around

Table 1
The maximum UV–vis absorption and fluorescence emission wavelengths.

Compound	UV–vis (nm)[a]	FL (nm)[b]
Dyad **1**	443, 416, 394, 339	451
Dyad **2**	447, 421,394, 338	448
Dyad **3**	447, 421, 397, 338	458
Perylene **4**[c]	437, 420, 392	452
TTF **7**	335	–

[a] UV–vis spectra were obtained at a concentration of 10^{-5} mol/L in CH_2Cl_2.
[b] Fluorescence spectra in CH_2Cl_2, λ_{exc} = 420 nm, $c = 10^{-5}$ mol/L.
[c] The UV–vis absorption of perylene **4** was measured in the same conditions as the dyads.

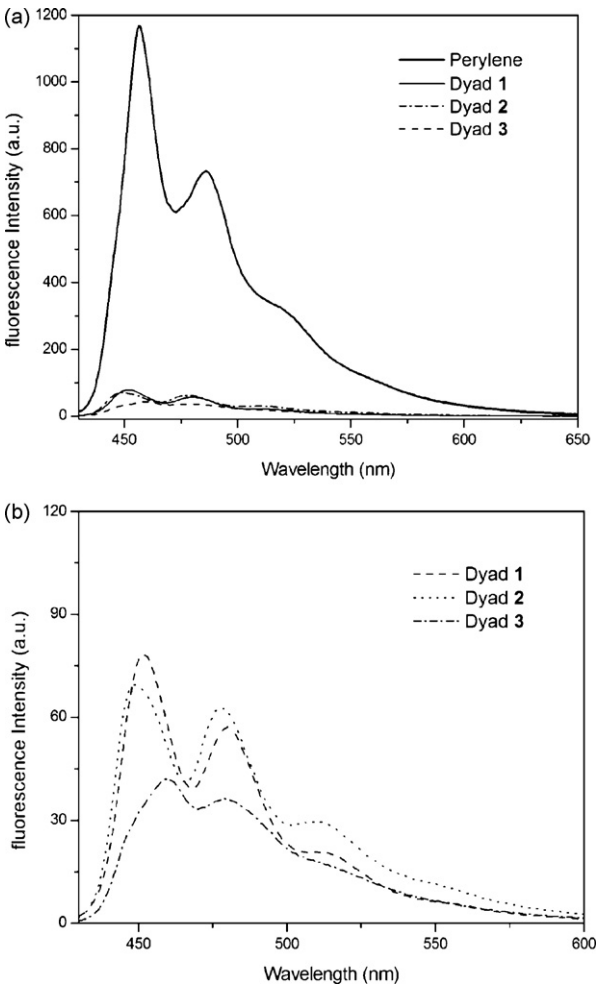

Fig. 4. (a) The fluorescence emission spectra of dyads **1–3** and perylene **4**, in CH_2Cl_2, λ_{exc} = 420 nm, $c = 1 \times 10^{-5}$ mol/L. (b) Fluorescence spectra of dyads **1–3** in CH_2Cl_2, λ_{exc} = 420 nm, $c = 1 \times 10^{-5}$ mol/L.

420 and 450 nm and a shoulder at 390 nm, which were attributed to the 20 π-electron perylene moiety. A weak absorption band around 340 nm was observed in Fig. 3 as well, which belonged to the absorption of the TTF moiety by comparing with the absorption curve of TTF **7**. No new absorption band or distinctive spectroscopic shoulder was detected in the UV–vis spectra, just the summation of the spectra of both TTF and perylene units. This fact suggested that no appreciable interaction between the TTF and perylene moieties in the ground states, in despite of the different σ-bonds linkage of dyads **1** and **2**. The spatial separation of electron donor and acceptor units was the main reason for the negligible intramolecular charge-transfer interaction in dyads, which was similar to the previous studies [17,25].

In addition, the absorption intensity of dyad **3** was higher than another two dyads in the region of 350–500 nm and the two perylene rings of the dyad **3** could be one reason. Comparing with dyad **2**, a slightly blue shift (4 nm) of maximum absorption wavelength for dyad **1** was observed, which was most probably caused by the electron withdrawing effect of the ester linkage.

3.3. Steady-state fluorescence and fluorescence lifetimes

The emission spectra of all the dyads were excited at λ_{exc} = 420 nm with perylene **4** as the reference, as shown in Fig. 4a. The maximum fluorescence wavelengths of the dyads were given in Table 1. Comparing with the fluorescence spectrum of perylene **4**, a strong fluorescence quenching for dyads **1–3** was observed (c.a. 90% for dyads **1** and **2**, and 95% for dyad **3**). As there was a smaller optical band gap of the perylene moiety than that of the TTF moiety, *i.e.* there was a minimal spectral overlap between the absorption spectrum of the TTF unit and fluorescence spectrum of the perylene fragment and according to the Förster mechanism, quenching caused by energy transfer process from perylene to TTF in the existed state would be prohibited [26]. Thus, the reason for the fluorescence quenching was most probably the photoinduced electron transfer (PET) interaction between the perylene and TTF moieties, and the PET process was thermodynamically favorable based on Rehm–Weller equation [27].

Table 2
The maximum absorption wavelengths λ_{max} (nm), molar extinction coefficients ε_{max} ($1\ mol^{-1}\ cm^{-1}$), fluorescence quantum yields Φ_f (λ_{exc} = 420 nm), radiative lifetimes τ_0 (ns) of dyads **1–3** in CH_2Cl_2.

Dyads	λ_{max}	ε_{max}	Φ_f	τ_0
1	443	34500	0.10	36
2	447	30500	0.11	37
3	447	47300	0.05	28

More fines of the fluorescence emission curves of dyads **1**, **2** and **3** were shown in Fig. 4b. All the fluorescence emission curves were mirror images of the curves of absorption of the dyads. Obviously, two fluorescence emission peaks at 450 and 480 nm arise from the excited singlet state of the perylene fragment. The emission curves of dyads **1** and **2** seemed similar, though different σ-bond linkages in them. The interaction between the perylene moieties was revealed by the corresponding fluorescence curve of dyad **3**, a Stokes' shift and a larger fluorescence quench were most probably caused by the interaction between the excited and unexcited perlyene moieties in dyad **3** in the excited state. The configuration interaction of the perylene moieties could also be deduced by the less structured fluorescence spectrum of the dyad **3** compared with those of dyads **1** and **2**.

The maximum absorption wavelengths λ_{max} (nm, CH_2Cl_2), fluorescence quantum yields Φ_f (the emission spectra of all dyads were taken at λ_{exc} = 420 nm with perylene **4** as the standard, $\Phi_{fP4} = 1$), radiative lifetimes τ_0 (ns) of the dyads were listed in Table 2. The theoretical radiative lifetimes τ_0 were calculated according to the formula: $\tau_0 = 3.5 \times 10^8/\nu^2_{max}\varepsilon_{max}\Delta\nu_{1/2}$, where ν_{max} stands for the wavenumber in cm^{-1}, ε_{max} for the molar extinction coefficient at the selected absorption wavelength and $\Delta\nu_{1/2}$ represented the half-width of the selected absorption in units of cm^{-1} [28].

The technique of time correlated single photon counting was used to record fluorescence lifetimes of the dyads, and the measured fluorescence lifetimes were offered (Table 3). The calculated fluorescence lifetimes $\tau_f' = \tau_0\Phi_f$ and the rate of fluorescence from $k_f = 1/\tau_f'$ were also given in Table 3.

The fluorescence lifetime of perylene **4** was measured for comparison and it was only a single-exponential decay with a fluorescence lifetime of 5.98 ns. In contrast, the fluorescence decay curves of dyads **1–3** were well-fitted double-exponential decay

Table 3
The measured fluorescence lifetimes τ_f (ns)[a], calculated fluorescence lifetimes τ_f' (ns), reduced χ^2 value and fluorescence rate constants k_f ($10^8\ s^{-1}$) of dyads **1–3** in CH_2Cl_2.

Dyads	τ_f	χ_2	τ_f'	k_f
1	1.05 (64.55%), 5.97 (35.45%)	1.107	3.6	2.7
2	1.52 (68.32%), 6.03 (32.68%)	1.002	4.1	2.5
3	0.64 (59.87%), 5.74 (40.13%)	1.092	1.3	7.7

[a] The measured fluorescence lifetimes were obtained in CH_2Cl_2, $c = 10^{-5}$ mol/L, E_{ex} = 372 nm, E_{em} = 450 nm, corresponding to the emission maxima of the perylene chromophore in CH_2Cl_2.

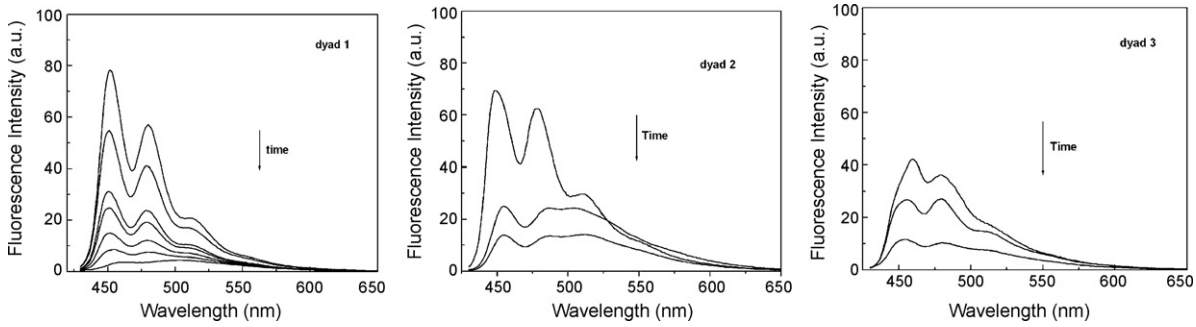

Fig. 5. Fluorescence emission spectra of dyads **1–3** recorded before and after addition of an excess of (diacetoxyiodo)benzene in the presence of triflic acid in CH_2Cl_2 ($c = 10^{-5}$ mol/L, $\lambda_{exc} = 420$ nm), the fluorescence emission curves were recorded every 5 min.

component and the reduced χ^2 values were given in Table 3. The fluorescence lifetimes of dyads **1–3** were all consisted of a fast major component and a decay minor component [29]. The two-component fluorescence lifetimes were expected to belong to the perylene unit itself and the interaction in the dyads in the excited state [30]. The longer fluorescence lifetime of the dyads was almost the same with that of the perylene monomer, while the relatively short-lived fluorescence lifetime could be assignable to the residual component after the photochemical communication between perylene cores and TTF units [31]. Comparing the measured fluorescence lifetimes of all the dyads, we could find the reduced tendency of fluorescence lifetimes was in good agreement with the fluorescence intensity reduction in CH_2Cl_2. The calculated fluorescence lifetimes of the dyads indicated the same reduced tendency (see Table 3).

3.4. Chemical oxidation

The fluorescence intensity of the dyads **1–3** was strongly quenched, theoretically speaking, if the TTF units in the dyads could be oxidized chemically or electrochemically, the photoinduced electron-transfer from TTF to perylene units could be hindered and the fluorescence intensity of the dyads would be recovered. However, when the neutral TTF was oxidized to the radical cation, the $TTF^{\bullet+}$ species had a broad absorption in the wavelength range of 350–600 nm [16,32], there would be a large spectral overlap between the absorption spectrum of the TTF radical cation and the fluorescence spectrum of the perylene unit. As a result, the photoinduced energy transfer could take place effectively between $TTF^{\bullet+}$ and the perylene unit and the fluorescence intensity might not be enhanced at this stage. But when the TTF was oxidized into radical dication, its absorption would be in the range of 600–800 nm [16], which was not overlap with the fluorescence spectrum of the perylene and the energy transfer would not take place. Thus the chemical oxidation experiments were carried out by adding excess of diacetoxyiodobenzene in the presence of triflic acid ($PhI(OAc)_2/CF_3SO_3H$) in CH_2Cl_2, as the neutral TTF could be oxidized into radical dication easily with the oxidant [33]. The fluorescence emission was recorded without any supplementary addition of oxidation reagent. Surprisingly, the fluorescence intensity of the dyads was quenched more deeply at the TTF^{2+}–perylene state (Fig. 5), which was totally different from the chemical oxidation results of the previous reported TTF–PDI molecular system [16]. We ascribed this phenomenon to a stronger binding between the two π-electron-rich units. A reverse photoinduced electron transfer and the intersystem crossing (ISC) interaction between the perylene fragment and TTF unit could respond for this. Based on the previous reports of PDI–TTF molecular systems [16,19,34], we considered that the reverse photoinduced electron transfer interaction should be the main contribution to this stronger quench. TTF dicationic species could be treated as electron acceptors [35] and the photo-excitation of the perylene might increase its acceptor strength, accompanied by an equal increase in its donor strength, thus perylene* could readily donate electrons to electron-deficient TTF^{2+} species and a new reverse electron transfer was existed. The similar phenomena were reported in a TTF–Pc system [32] and a TTF–anthracene polymer [36]. For dyads **1–3**, the photoinduced reverse electron-transfer kinetic process should be much more efficient because the fluorescence intensity was quenched ever than before.

The fluorescence intensity reached a minimize value after about 30 min for dyad **1** and 10 min for dyads **2** and **3**, it implied that the intramolecular electron-transfer interaction in dyads **2** and **3** were occurred more easily than dyad **1**.

3.5. Electrochemistry

The electrochemical redox properties of dyads **1–3** were studied by cyclic voltammetry (CV) in CH_2Cl_2 (Table 4). The CV data of perylene **4**, TTFs **6** and **7** were also presented in Table 4 as reference. All the dyads exhibited a wide one-electron irreversible reduction wave in the negative position, indicating the reduction of the perylene moiety to $perylene^{\bullet-}$. The sequent reduction of the perylene moiety was not observed in CH_2Cl_2 containing 0.1 M n-Bu_4NPF_6. Two reversible TTF oxidation waves, one reversible perylene oxidation wave and one irreversible perylene oxidation wave were shown in the positive direction, corresponding to the radical cation $TTF^{\bullet+}$–perylene, dication TTF^{2+}–perylene, TTF^{2+}–$perylene^{+}$ and TTF^{2+}–$perylene^{2+}$, respectively.

Comparing TTFs **6** with **7**, the electron-withdrawing substitute on the TTF **6** made oxidation of TTF unit less favorable and the anodic shift was observed, which was also existed in the TTF–perylene dyads. In the case of dyad **3**, the presence of the two electron-withdrawing perylene rings reduced the electron-donating ability of the TTF fragment more strongly, leading to the positive shift of the TTF oxidation wave and increased the electrochemistry HOMO–LUMO gap [13]. As the perylene moiety and the TTF moiety

Table 4
Electrochemical data for dyads **1**, **2** and **3**, perylene **4**, TTFs **6** and **7** in CH_2Cl_2[a,b].

Compounds	E_{red1} (V)	E_{ox1} (V)	E_{ox2} (V)	E_{ox3} (V)	E_{ox4} (V)
Dyad **1**	−1.58	0.62	1.01	1.23	1.68
Dyad **2**	−1.59	0.62	0.99	1.24	1.72
Dyad **3**	−1.75	0.65	1.00	1.23	1.70
Perylene **4**	−1.82				
TTF **6**		0.65	1.01		
TTF **7**		0.60	0.99		

[a] The values (V) were recorded in CH_2Cl_2 solution using n-Bu_4NPF_6 0.1 M in CH_2Cl_2 as supporting electrolyte, AgCl/Ag as the reference electrodes, platinum wires as counter and working electrodes, scan rate: 50 mV/s.

[b] Versus AgCl/Ag.

Table 5
The calculated HOMO, LUMO orbital energies, ΔE^{cv} and $\Delta E^{0-0} = 1240/\lambda$.

Dyads	E_{HOMO} (eV)	E_{LUMO} (eV)	ΔE^{cv} (eV)	ΔE^{0-0} (eV)
1	−5.32	−3.12	2.20	2.74
2	−5.32	−3.11	2.21	2.72
3	−5.35	−2.95	2.40	2.74

in the dyads showed their individual electrochemical characteristics, it exhibited that neither intermolecular nor intramolecular interaction took place between the electroactive moieties in the ground state and the result was matched that of the UV–vis absorption. The HOMO orbital and LUMO orbital energies (eV) were calculated from cyclic voltammograms based on the value of 4.7 eV for Fc (Table 5). The optical band gap $\Delta E^{0-0} = 1240/\lambda$ were given in the table as comparison.

Optimized structures of dyads **1–3** were presented in Fig. 6. For dyads **1** and **2**, with flexible chain, the extended structure had minimum potential energy. Two long alkyl chains were extended to different orientations of the TTF plane. The structure difference between **1** and **2** was due to the orientation of the methyl on the TTF moiety. In dyad **1**, the perylene unit of the opposite position to the methyl seemed to have the optimized structure and the dihedral angel of the two planes was evaluated to be smaller. For dyad **3**, two perylene planes had different orientations with respect to the TTF moiety and almost paralleled with the TTF fragment. The calculation of electron densities of the HOMO and LUMO for dyads **1–3** revealed the LUMO localized on the perylene moieties, corresponding to the distribution of the electron (radical anion) in the charge-separated state. However, the HOMO localized partly on the TTF fragments and mostly still localized on the perylene fragments, which corresponds to the distribution of the hole (radical cation) in the charge-separated state. The results indicated that in dyads **1–3**, there was no intramolecular interaction in the ground state, which matched the absorption spectra and CV results.

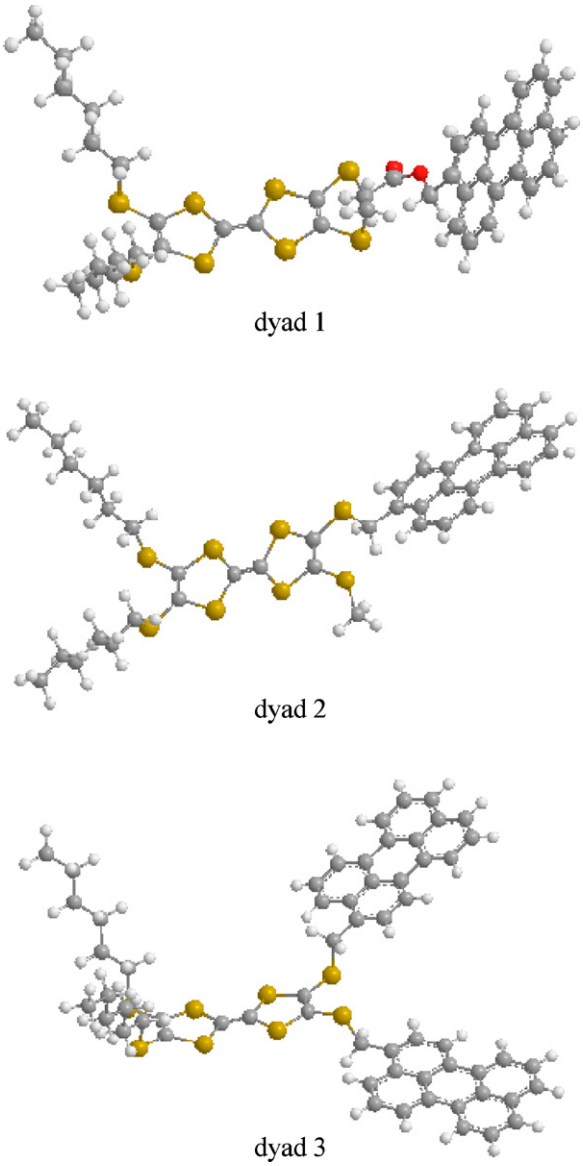

Fig. 6. Optimized molecular structures of dyads **1–3**.

4. Conclusions

Three TTF–perylene dyads, linked by two kinds of covalent bridges, were synthesized and characterized. The absorption spectra of dyads in CH_2Cl_2 were the addition of perylene and TTF units, indicating no intramolecular charge transfer interaction in their ground state. The photoinduced electron transfer interactions in dyads **1–3** were rationalized based on the fluorescence spectra and theoretical calculation. The redox of the dyads revealed no obvious shift compared to the individual TTF and perylene, which also indicated no internal charge transfer interaction occurred in their ground state. Quantum mechanical calculation gave the energy optimal structures of dyads **1–3** and the frontier orbital calculation implied there was no intramolecular charge transfer interaction in the ground state. With the chemical oxidation experiment of the dyads to the TTF^{2+}–perylene state, a fast and effective electron transfer in the reverse direction to that of the unoxidized TTF–perylene dyads was undergoing and a facile method of reversing electron transfer within a donor–acceptor system was presented. The difference in covalent bridges had little influence on the photo- and electrochemical properties of the TTF–perylene molecular systems.

Acknowledgements

This work was supported by National Natural Science Foundation of China (no.20676036) and the Key Project of the Ministry of Education of China (no. 03053).

References

[1] H. Icil, E. Arslan, Synthesis and spectroscopic properties of highly pure perylene fluorescent dyes, Spectrosc. Lett. 34 (2001) 355–363.
[2] H. Icil, D. Uzun, E. Arslan, Synthesis and spectroscopic characterization of water soluble perylene tetracarboxylic diimide derivatives, Spectrosc. Lett. 34 (2001) 605–614.
[3] J.M. Serin, D.W. Brousmiche, J.M.J. Fréchet, Cascade energy transfer in a conformationally mobile multichromophoric dendrimer, Chem. Commun. (2002) 2605–2607.
[4] T. Weil, J.Q. Qu, K. Müllen, Towards U. Rohr, K. Kohl, K. Müllen, A. Craats, J. Warman, Liquid crystalline coronene derivatives, J. Mater. Chem. 11 (2001) 1789–1799.
[5] K. Kohl, Highly fluorescent and water-soluble perylene dyes, Chem. Eur. J. 10 (2004) 5297–5310.
[6] F. Würthner, Z.J. Chen, V. Dehm, V. Stepanenko, One-dimensional luminescent nanoaggregates of perylene bisimides, Chem. Commun. (2006) 1188–1190.
[7] P. Bauer, H. Wietasch, S.M. Lindner, M. Thelakkat, Synthesis and characterization of donor-bridge-acceptor molecular containing tetraphenylbenzidine and perylene bisimide, Chem. Mater. 19 (2007) 88–94.
[8] P. Schlichting, U. Rohr, K. Müllen, New synthetic routes to alkyl-substituted and functionalized perylenes, Liebigs Ann. (1997) 395–407.
[9] Y. Nagao, T. Naito, Y. Abe, T. Misono, Synthesis and properties of long and branched alkyl chain substituted perylenetetracarboxylic monoanhydride monoimides, Dyes Pigments 32 (1996) 71–83.
[10] C. Goze, S.X. Liu, C. Leiggener, L. Sanguinet, E. Levillain, A. Hauser, S. Decurtins, Synthesis of new ethynylbipyridine-linked mono- and bis-tetrathiafulvalenes:

electrochemical, spectroscopic, and Ru(II)-binding studies, Tetrahedron 64 (2008) 1345–1350.
[11] J.L. Segura, N. Martin, New concepts in tetrathiafulvalene chemistry, Angew. Chem. Int. Ed. 40 (2001) 1372–1409.
[12] H.C. Li, J.O. Jeppesen, E. Levillain, J. Becher, A mono-TTF-annulated porphyrin as a fluorescence switch, Chem. Commun. (2003) 846–847.
[13] J.C. Wu, S.X. Liu, A. Neels, F.L. Derf, M. Sallé, S. Decurtins, A tetrathiafulvalene–tetracyanoanthraquinodimethane (TTF–TCNAQ) diad with a chemically tunable HOMO–LUMO gap, Tetrahedron 63 (2007) 11282–11286.
[14] G.X. Zhang, D.Q. Zhang, X.F. Guo, D.B. Zhu, A new redox-fluorescence switch based on a triad with tetrathiafulvalene and anthrancene units, Org. Lett. 6 (2004) 1209–1212.
[15] Z. Wang, D.Q. Zhang, D.B. Zhu, A new saccharide sensor based on a tetrathiafulvalene-anthrancene dyad with a boronic acid group, J. Org. Chem. 70 (2005) 5729–5732.
[16] S. Leroy-Lhez, J. Baffreau, L. Perrin, E. Levillain, M. Allain, M.-J. Blesa, P. Hudhomme, Tetrathiafulvalene in a perylene-3,4:9,10-bis(dicarboximide)-based dyad: a new reversible fluorescence-redox dependent molecular system, J. Org. Chem. 70 (2005) 6313–6320.
[17] X.F. Guo, D.Q. Zhang, H.J. Zhang, Q.H. Fan, W. Xu, X.C. Ai, L.Z. Fan, D.B. Zhu, Donor-acceptor-donor triads incorporating tetrathiafulvalene and perylene diimide units: synthesis, electrochemical and spectroscopic studies, Tetrahedron 59 (2003) 4843–4850.
[18] M.J. Frisch, G.W. Trucks, H.B. Schlegel, G.E. Scuseria, M.A. Robb, J.R. Cheeseman, J.A. Montgomery, Jr., T. Vreven, K.N. Kudin, J.C. Burant, J.M. Millam, S.S. Iyengar, J. Tomasi, V. Barone, B. Mennucci, M. Cossi, G. Scalmani, N. Rega, G.A. Petersson, H. Nakatsuji, M. Hada, M. Ehara, K. Toyota, R. Fukuda, J. Hasegawa, M. Ishida, T. Nakajima, Y. Honda, O. Kitao, H. Nakai, M. Klene, X. Li, J.E. Knox, H.P. Hratchian, J.B. Cross, V. Bakken, C. Adamo, J. Jaramillo, R. Gomperts, R.E. Stratmann, O. Yazyev, A.J. Austin, R. Cammi, C. Pomelli, J.W. Ochterski, P.Y. Ayala, K. Morokuma, G.A. Voth, P. Salvador, J.J. Dannenberg, V.G. Zakrzewski, S. Dapprich, A.D. Daniels, M.C. Strain, O. Farkas, D.K. Malick, A.D. Rabuck, K. Raghavachari, J.B. Foresman, J.V. Ortiz, Q. Cui, A.G. Baboul, S. Clifford, J. Cioslowski, B.B. Stefanov, G. Liu, A. Liashenko, P. Piskorz, I. Komaromi, R.L. Martin, D.J. Fox, T. Keith, M.A. Al-Laham, C.Y. Peng, A. Nanayakkara, M. Challacombe, P.M.W. Gill, B. Johnson, W. Chen, M.W. Wong, C. Gonzalez, J.A. Pople, Gaussian 03, Revision D.01, Gaussian Inc., Wallingford CT, 2004.
[19] K.B. Simonsen, N. Svenstrup, J. Lau, O. Simonsen, P. MΦrk, G.J. Kristensen, J. Becher, Sequential functionalisation of bis-protected tetrathiafulvalene-dithiolates, Synthesis 3 (1996) 407–418.
[20] N. Svenstrup, K.M. Rasmussen, T.K. Hansen, J. Becher, The chemistry of TTFTT; 1: new efficient synthesis and reactions of tetrathiafulvalene-2,3,6,7-tetrathiolate (TTFTT): an important building block in TTF-syntheses, Synthesis 8 (1994) 809–812.
[21] C.A. Christensen, M.R. Bryce, J. Becher, New multi(tetrathiafulvalene) dendrimers, Synthesis 12 (2000) 1695–1704.
[22] M.V. Skorobogatyi, A.A. Pchelintseva, A.L. Petrunina, I.A. Stepanova, V.L. Andronova, G.A. Galegov, A.D. Malakhov, V.A. Korshun, 5-Alkynyl-2′-deoxyuridines, containing bulky aryl groups: evaluation of structure-anti-HSV-1 activity relationship, Tetrahedron 62 (2006) 1279–1287.
[23] I.V. Grechishnikova, L.B.A. Johansson, J.G. Molotkovsky, Synthesis of new bifluorophoric probes adapted to studies of donor-donor electronic energy transfer in lipid systems, Chem. Phys. Lipids 81 (1996) 87–98.
[24] K. Heuzé, M. Fourmigué, P. Batail, The crystal chemistry of amide-functionalized ethylenedithiotetrathiafulvalenes: EDT-TTF-CONRR′ (R, R′∼H, Me), J. Mater. Chem. 9 (1999) 2373–2379.
[25] X.F. Guo, Z.H. Gan, H.X. Luo, Y. Araki, D.Q. Zhang, D.B. Zhu, O. Ito, Photoinduced electron-transfer processes of tetrathiafulvalene-(spacer)-(naphthalenediimide)-(spacer)-tertrathiafulvalene triads in solution, J. Phys. Chem. A 107 (2003) 9747–9753.
[26] R. Gómez, C. Coya, J.L. Segura, Synthesis of a π-extended TTF-perylenediimide donor-acceptor dyad, Tetrahedeon Lett. 48 (2008) 3225–3228.
[27] The corresponding free energies (ΔG_{PET}) were estimated using the Rehm–Weller equation. D. Rehm, A. Weller, Irs. J. Chem. 8 (1970) 259–265. $\Delta G_{PET} = E_{(ox)} - E_{(red)} - E^{0-0}(\text{dyad}) - \Delta e$. For dyad **1**: with $E_{(ox)} = +0.62$ eV, $E_{(red)} = -1.58$ eV, $E^{0-0}(\mathbf{1}) = 2.74$ eV, $\Delta e \approx 0.1$ eV, the value of ΔG_{PET} is -0.54 eV; dyad **2**: with $E_{(ox)} = +0.62$ eV, $E_{(red)} = -1.59$ eV, $E^{0-0}(\mathbf{2}) = 2.72$ eV, $\Delta e \approx 0.1$ eV, the value of ΔG_{PET} is -0.51 eV; dyad **3**: with $E_{(ox)} = +0.65$ eV, $E_{(red)} = -1.75$ eV, $E^{0-0}(\mathbf{3}) = 2.74$ eV, $\Delta e \approx 0.1$ eV, the value of ΔG_{PET} is -0.34 eV. These values estimate the PET interaction is thermodynamically favorable.
[28] H. Langhals, L. Feiler, Pyrroli and thiophenoperylenedicarboximides highly fluorescent heterocycles, Liebigs Ann. (1996) 1587–1591.
[29] Y. Zhang, Z. Xu, L. Cai, G. Lai, H. Qiu, Y. Shen, Highly soluble perylene tetracarboxylic diimides and tetrathiafulvalene-perylene tetracarboxylic diimide-tetrathiafulvalene triads, J. Photochem. Photobiol. A: Chem. 200 (2008) 334–345.
[30] J. Ren, X. Zhao, Q. Wang, C. Ku, D. Qu, C. Chang, H. Tian, Synthesis and fluorescence properties of novel co-facial folded naphthalimide dimers, Dyes Pigments 64 (2005) 179–186.
[31] P. Du, W. Zhu, Y. Xie, F. Zhao, C. Ku, Y. Cao, C. Chang, H. Tian, Dendron-functionalized macromolecules: enhancing core luminescence and tuning carrier injection, Macromolecules 37 (2004) 4387–4398.
[32] C. Farren, C.A. Christensen, S. FitzGerland, M.R. Bryce, A. Beeby, Synthesis of novel phthalocyanine-tetrathiafulvalene hybrids; intermolecular fluorescence quenching related to molecular geometry, J. Org. Chem. 67 (2002) 9130–9139.
[33] M. Giffard, G. Mabon, E. Leclair, N. Mercier, M. Allain, A. Gorgues, P. Molinié, O. Neilands, P. Krief, V. Khodorkovsky, Oxidation of TTF derivatives using (diacetoxyiodo)benzene: a general chemical route toward cation radicals, dications, and nonstoichiometric salts, J. Am. Chem. Soc. 123 (2001) 3852–3853.
[34] Y. Zhang, L. Cai, C. Wang, G. Lai, Y. Shen, Synthesis and properties of a tetrathiafulvalene–perylene tetracarboxylic diimide–tetrathiafulvalene dyad, New J. Chem. 32 (2008) 1968–1973.
[35] P.R. Ashton, V. Balzani, J. Becher, A. Credi, M.C.T. Fyfe, G. Mattersteig, S. Menzer, M.B. Nielsen, F.M. Raymo, J.F. Stoddart, M. Venturi, D.J. Williams, A three-pole supramolecular switch, J. Am. Chem. Soc. 121 (1999) 3951–3957.
[36] H.A. De Cremiers, G. Clavier, F. Ilhan, G. Cooke, V.M. Rotello, Tuneable electrochemical interactions between polystyrenes with anthracenyl and tetrathiafulvalenyl sidechains, Chem. Commun. (2001) 2232–2233.